ELSEVIER

Thin Solid Films 313–314 (1998) 137–142

thin solid films

Development of a parametric optical constant model for $Hg_{1-x}Cd_xTe$ for control of composition by spectroscopic ellipsometry during MBE growth

B. Johns[a,*], C.M. Herzinger[a], J.H. Dinan[b], A. Cornfeld[b], J.D. Benson[b]

[a] *J.A. Woollam Co, Suite 102, 645 M St., Lincoln, NE 68508, USA*
[b] *US Army CECOM Night Vision and Electronic Sensors Directorate, Ft. Belvoir, VA, USA*

Abstract

The development of an optical constant library for $Hg_{1-x}Cd_xTe$ as a function of composition ($x = 0$–0.5) and temperature ($T = 0$–250°C) which is suitable for precise composition control by spectroscopic ellipsometry (SE) during MBE growth is described. An efficient methodology for acquiring in situ optical constants as a function of composition and temperature is first presented. Optical constants extracted from these in situ measurements, as well as literature data from room temperature values, were used to obtain internally Kramers-Kronig consistent parametric optical constant models at discrete compositions and temperatures. Then a global data analysis over temperature 'T' and composition 'x' was performed in which the internal parameters of the optical constant model were fitted as polynomials in T and x. This parametric model was developed to replace, without compromising the quality of ellipsometric data fits, the usual tabulated optical constant lists while using a reasonably small set of adjustable parameters. The model is flexible enough to describe the complicated critical point structures of semiconductors, yet stable enough to generate optical constants as a function of composition and temperature and permit limited extrapolation outside the measured range. © 1998 Elsevier Science S.A.

Keywords: Ellipsometry; Optical constants; HgCdTe; In situ characterization

1. Introduction

To perform real-time monitoring of composition during MBE growth by spectroscopic ellipsometry (SE), a highly accurate and systematic optical constant library which can generate spectra as a function of both composition and temperature is required. The library must encompass the composition and temperature range which would be normally encountered during growth, and it would even be desirable to extrapolate outside this range, in order to detect and diagnose anomalous growth conditions. This work describes the development of such an optical constant library, which is basically divided into two aspects: (1) in situ measurement of optical constants, and (2) building a parameterized composition- and temperature-dependent optical constant library. Another important aspect of developing an optical constant library is validation, which is discussed in a companion paper in this proceedings [1].

2. Measurement of in situ optical constants

Ideally, one would like to determine exact, intrinsic, optical constant spectra for the semiconductor system of interest for the complete range of growth temperatures and compositions, by performing in situ SE measurements during a systematic series of growth

* Corresponding author. Tel.: +1 402 4777501; fax: +1 402 4778214; e-mail: bjohs@jawoollam.com

PII S0040-6090(97)00800-6

runs. The layer compositions and/or temperatures for each run would be known and independently verified by non-ellipsometric means such that accurate values could be associated with each measured optical constant spectra. Unfortunately, this objective is not achievable in a reasonable time frame, as it would typically require a separate growth run and ex situ analysis for each composition. Building an optical constant library across multiple growth runs also tends to introduce some inconsistency into the constituent optical constant spectra, due to potential variations in the ellipsometer angle of incidence, growth temperature, and surface quality.

It is more realistic to determine optical constant spectra for a semiconductor ternary system of interest at a few temperatures in the typical growth regime of the system, and at a limited number of representative compositions. Furthermore, only nominal values for temperature and composition need to be assigned to the measured spectra initially. These nominal values may not be accurate in an absolute sense, but they will enable the reproducible in situ determination of temperature and composition at least in a relative sense. The nominal values for temperature and composition can later be replaced by more accurate values when that information becomes available (e.g. through extensive ex situ analysis). Thus, without remeasuring the optical constants, the accuracy can always be fine tuned assuming the precision is good enough. Reproducibility (relative accuracy) is more important and more readily achievable than absolute accuracy, which can still be developed over time.

The following general growth procedure can be used to measure optical constants at nominal temperatures $t_x = t_1 \cdots t_n$ and compositions $c_y = c_1 \cdots c_m$. (1) The wafer temperature is ramped to remove the oxide and a thick buffer layer (ideally a binary) is grown to provide a smooth, high-quality surface. During the buffer layer growth, the wafer temperature should be stabilized and maintained at t_1. (2) The temperature is stabilized at t_x and a layer of composition c_y is grown. A layer thickness greater than the $1/4$ wave optical thickness of the material should be grown. Because the optical constants are different from the buffer layer, interference effects will be observed in the ellipsometric data. By performing a growth-rate analysis on these data, highly accurate optical constants of the growing layer can be determined, even when the layer is grown on top of a complex multilayer structure. For many material systems, the growth rates of the test layers can be correlated with the source fluxes to provide a good estimate of the composition after making certain assumptions about the sticking coefficients. By analyzing the measured data at many times (different thicknesses) the data analysis becomes over-determined, and it is possible to minimize inaccuracies from ellipsometer errors, material interfaces, and surface non-idealities. (3) A buffer layer is grown (again greater than $1/4$ wave optical thickness) with the temperature remaining stabilized at t_x. During this growth, the sources setting the composition can be ramped and stabilized for the next composition of interest. Also, optical constants can be extracted from the buffer layer. Comparing the results from the multiple buffer layers provides a good self-consistency check of the temperature stability and potential optical constant accuracy. With the buffer layer grown there is now optical contrast for growing the next layer of interest. (4) Steps 2 and 3 are repeated 'm' times for each composition c_y. (5) Steps 2–4 are repeated 'n' times for each temperature t_x. (The total number of temperature- and composition-dependent optical constant spectra which are acquired in this approach is '$n \times m$'.)

There are several advantages of this procedure. It can be used (with some possible modifications) with almost any lattice matched or nearly matched ternary semiconductor system and with different growth techniques (MBE, MOVPE, etc.). The optical constants are determined during a single growth run, eliminating problems with reproducing the angle of incidence and temperatures. The procedure is simple enough that it can be performed on different growth chambers to assess potential differences. The optical constants obtained from observation of the dynamic growing surface may also be more accurate (and useful) than from a static surface.

The above methodology was applied to the MBE growth of $Hg_{1-x}Cd_xTe$. A VG V80H MBE chamber, and a commercially available in situ SE system [2], was used for this work. To acquire $Hg_{1-x}Cd_xTe$ optical constant data, a single growth run was performed at a single temperature and five compositions. (The growth structure is shown in Table 1, and in situ SE data acquired during the run are presented in Fig. 1.) Only a single growth temperature was used for the following reasons: (1) with current technology, high quality MBE growth of HgCdTe occurs only in a very narrow temperature window (180–190°C); it is difficult enough to keep within that window, and impractical to grow at multiple temperatures, and (2) the change in optical constants over 10° would be quite small anyway, and it was decided to use published room temperature optical constants [11] to complete the temperature dependence.

The dielectric functions extracted from the growth rate analysis of the SE data are shown in Fig. 2. The resulting HgCdTe optical constants exhibit low noise

Table 1
Multi-layer HgTe/$Hg_{1-x}Cd_xTe$ structure grown to determine composition-dependent optical constants at a single growth temperature

Nominal layer composition	Nominal layer thickness (Å)	CdTe cell temperature	Ellipsometer growth rate (Å/s)
HgCdTe $x = 0.32$	10 000	644°C	4.28
HgTe	2000	—	3.03
HgCdTe $x = 0.27$	10 000	638°C	4.12
HgTe	2000	—	3.05
HgCdTe $x = 0.17$	10 000	626°C	3.71
HgTe	2000	—	3.06
HgCdTe $x = 0.22$	10 000	632°C	3.92
HgTe	2000	—	3.09
HgCdTe $x = 0.22$	10 000	632°C	3.94
CdZnTe substrate	—	—	—

and are systematic, especially through the important E_1 and $E_1 + \Delta_1$ region from 2 to 3 eV. The reproducibility of the HgTe optical constants (Fig. 2) and growth rates (shown in Table 1) are very good.

3. Parametric optical constant model

There have been many parametric models published to represent optical constants in different spectral regions. However, none of them have the flexibility or internal formulation needed to fit optical constants over broad spectral regions from ellipsometric data acquired on multi-layer samples. For example, Adachi's model [3] works best for alloy systems in the region below the fundamental bandgap. Oscillator ensembles [4,5] only work above the fundamental gap and are difficult to extend to alloys (especially for extrapolation) because of the need for 'fictitious' oscillators to fill in the absorption between critical points. Forouhi and Bloomer published a model [6] that with improvements by McGahan [7] and Jellison [8] works for amorphous materials, but it lacks the flexibility to reproduce the sharp feature of crystalline semiconductors especially around a direct bandgap. Kim and Garland developed a Kramers-Kronig consistent model [9,10] which can describe a semiconductor's dielectric function and higher order derivatives. However the fitting procedure is a two stage process, there is substantial internal parameter correlation, and the Gaussian broadening needed to correctly model the transparency of a semiconductor below the bandgap is only approximated. The parametric model applied to this $Hg_{1-x}Cd_xTe$ work uses Gaussian broadening and polynomials for the absorption basis functions. In these respects, the model is somewhat like Kim and Garland's work, however, in this work the polynomials are centered around critical points rather than spanning between them, the Gaussian broadening is more accurately modeled, and the underlying shape parameters have been defined in a scale-independent manner to permit more stable shifting across composition and temperature ranges.

Analytically the dielectric function is written as the summation of 'm' energy-bounded, Gaussian-broadened polynomials and P poles accounting for index effects due to absorption outside the model region:

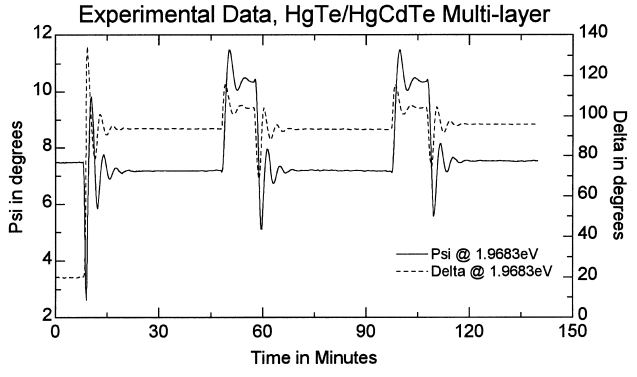

Fig. 1. In situ SE data acquired during MBE growth of the HgTe/HgCdTe multi-layer described in Table 1. The data shown correspond to the first five layers listed in Table 1.

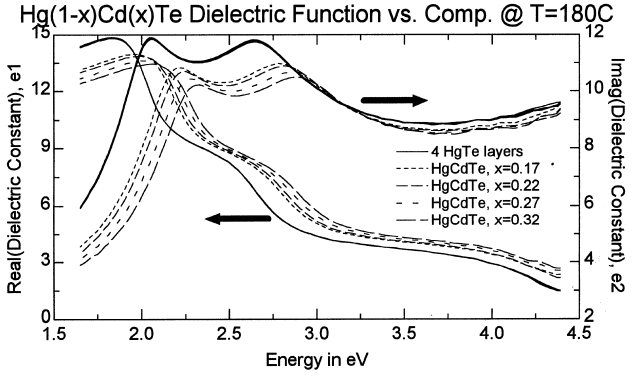

Fig. 2. Dielectric spectra for the four HgCdTe layers of different compositions and four HgTe layers of the multi-layer structure given in Table 1.

$$\varepsilon(\omega) = \varepsilon_1(\omega) + i\varepsilon_2(\omega) = 1 + i\sum_{j=1}^{m}\int_{E_{\min}}^{E_{\max}} W_j(E) \times \Phi(\hbar\omega, E, \sigma_j)\mathrm{d}E + \sum_{j=m+1}^{m+P+1} \frac{A_j}{(\hbar\omega)^2 - E_j^2} \text{where} \quad (1)$$

$$\Phi(\hbar\omega, E, \sigma) = \int_0^\infty e^{i(\hbar\omega - E + i2\sigma^2 s)s}\mathrm{d}s - \int_0^\infty e^{i(\hbar\omega + E + i2\sigma^2 s)s}\mathrm{d}s \quad (2)$$

$$= \sqrt{\frac{\pi}{8\sigma^2}}\left[e^{-y_1^2} + e^{-y_1^2}\mathrm{erf}(iy_1) - e^{-y_2^2} - e^{-y_2^2}\mathrm{erf}(iy_2)\right],$$

$$y_1 = \frac{\hbar\omega - E}{2\sqrt{2}\,\sigma} \quad \text{and} \quad y_2 = \frac{\hbar\omega + E}{2\sqrt{2}\,\sigma} \quad (2b)$$

$$W_j(E) = \sum_{k=0}^{N} P_{j,k}E^k u(E - a_j)u(b_j - E),$$

where $u(x)$ is the unit step function. (3)

A detailed explanation of these expressions is beyond the scope of this paper, and will be published elsewhere. The use of pure Gaussian broadening in Eq. (2) essentially prohibits closed form integration of Eq. (1). However, the equivalent expression shown in Eq. (2b) shows that one dimensional lookup tables as a function of $(\hbar\omega + E)/(2\sqrt{2}\,\sigma)$ can be numerically constructed for each order of polynomial required by Eq. (3). (This significantly reduces the computation time required to evaluate the model.)

In the specific implementation for this work, the polynomials are grouped into four polynomial ensembles which are centered on critical point structures with the overlapping tails of adjacent ensembles filling in the absorption, as depicted in Fig. 3. (Fourth order polynomials were used, corresponding to $N = 4$ in Eq. (3).) Thus there is no need for 'fictitious' oscillators which serve only to fill in gaps as required when using Lorentz or harmonic oscillator models. The center (E_C), bounding energies (E_L and E_U), and center amplitude (A) are specified absolutely. The position of the control points, which correspond to the joining points of the four polynomials, are defined relative to these absolutes. (For example, $E_{LM} = E_L + 0.7(E_C - E_L)$, and $A_{LM} = 0.3A_L$.) Thus a critical point ensemble can be moved to different energies or its amplitude can be changed without altering its shape significantly. This simplifies the task of fitting optical constant spectra over multiple compositions and temperatures, which requires a systematic shifting of the critical points. The polynomials are limited by the constraints that they are continuous in the zeroth, first, and second derivatives at the control points, that they go to zero at the bounding energies, and that outside polynomials are no more than second order. At the center energy, discontinuities in amplitude and energy are permitted; hence the two sides of the ensemble are independent and step-like absorption features can be created to model direct bandgaps.

4. HgCdTe optical constant library

Using the in situ data for nominal compositions of $x = 0$, 0.17, 0.22, 0.27, and 0.32 from Sec. 2 (which were acquired at a growth temperature of 180°C) and room temperature $Hg_{1-x}Cd_xTe$ optical constants at $x = 0$ and 0.20 [11], a global parametric fit was performed. In so doing, the energies, amplitudes, and control point parameters were permitted to become two dimensional polynomials of composition (x) and temperature (T). (Second order polynomials were used for the composition dependence, while first order polynomials were used for the temperature dependence, as only two temperatures were included in the analysis.) This was done over the more limited

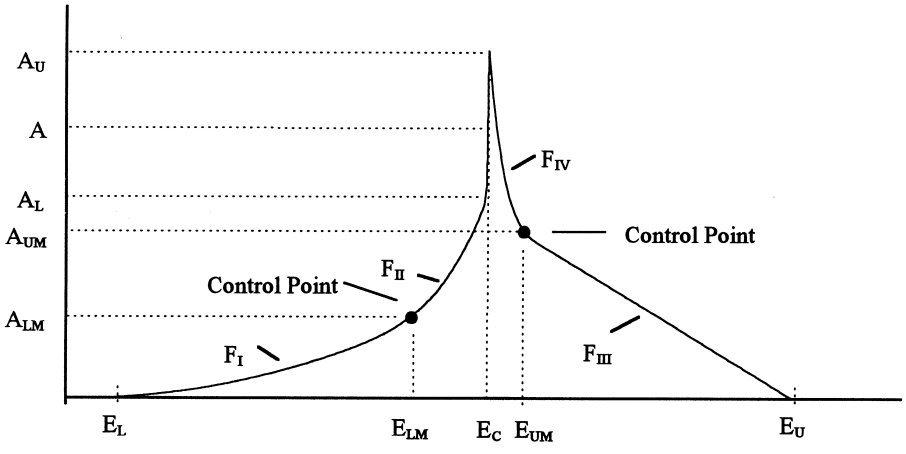

Fig. 3. A generic, unbroadened CP structure composed of four component polynomials, F_I, F_{II}, F_{III}, and F_{IV}.

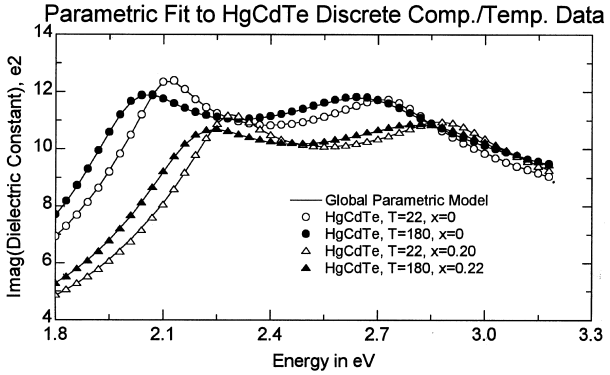

Fig. 4. Global parametric model fit to the discrete $Hg_{1-x}Cd_xTe$ optical constant spectra. (For clarity, only four of the seven constituent spectra used in the global analysis are shown. Only the imaginary part of the dielectric function is shown; due to Kramers-Kronig consistency, the fit to the real part of the dielectric function is comparable.)

spectral range of 1.8–3.4 eV which contains the critical point structures which are most sensitive to composition. The results of the fit are shown in Fig. 4.

Note that an evenly spaced grid of compositions and temperatures is not required to build this global model. However, for later in situ control where computation speed is at a premium, a tabulated version of the global model was created on a regular grid spanning temperatures of 0° to 250°C and compositions from $x = 0$ to 0.5. Short of experimental verification, there is no real way to know if the extrapolated region is accurate but one can at least assess the results for obvious impossibilities, such as the appearance of non-physical critical point features. In Fig. 5, the $Hg_{1-x}Cd_xTe$ optical constants vs. temperature for $x = 0.20$ were generated by the parametric model. Note that the curves follow systematic, plausible trends even though only data at 25°C and 180°C were used in the construction of the model. In Fig. 6, the generated composition spectra for $T = 190$°C are shown. These curves also show a plausible trend,

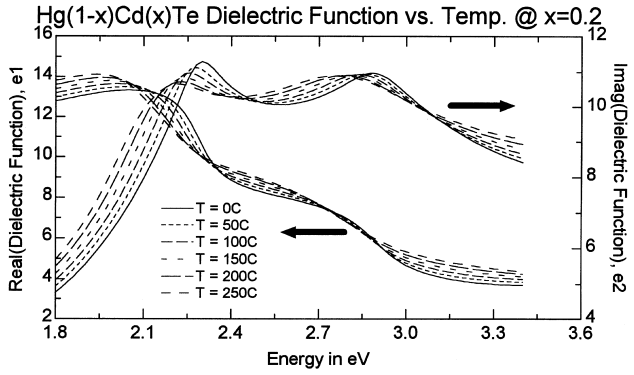

Fig. 5. $Hg_{1-x}Cd_xTe$ optical constant spectra as a function of temperature, extrapolated from the parametric model.

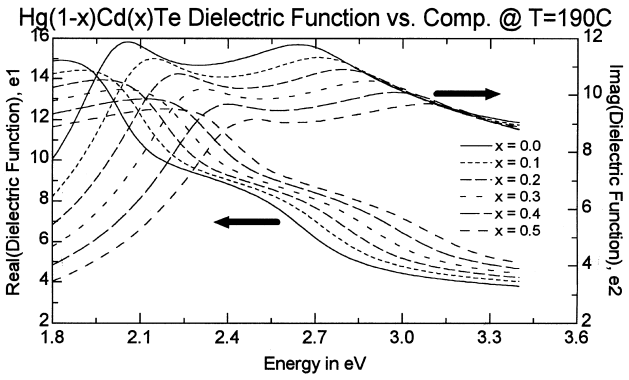

Fig. 6. $Hg_{1-x}Cd_xTe$ optical constant spectra as a function of composition, extrapolated from the parametric model.

which again underscores the ability of the global parametric model to provide a systematic, physical representation of the material optical constants.

5. Conclusions

A systematic procedure for acquiring composition- and temperature-dependent optical spectra has been described, and applied to the $Hg_{1-x}Cd_xTe$ material system. These spectra were globally fit by a Kramers-Kronig consistent parametric model, in which the parameters were a function of composition and temperature. From this global parametric model, an arbitrary grid of optical constant spectra versus composition and temperature were generated. Due to the stable nature and Kramers-Kronig consistency of the global parametric model, it was possible to extrapolate optical constant spectra outside the measured range. This ability can greatly improve the robustness of real-time composition monitoring by in situ spectroscopic ellipsometry.

Acknowledgements

This work was supported by US Army SBIR Contract DAAB-7-93-C-U008.

References

[1] B. Johs et al., Thin Solid Films 313–314 (1998) 490.
[2] M-88 in situ SE system (280–760 nm spectral range), J.A. Woollam Co., Lincoln, NE, USA.
[3] S. Adachi, Phys. Rev. B 38 (1988) 12345.
[4] M. Erman, J.B. Theeten, P. Chambon, S.M. Kelso, D.E. Aspnes, J. Appl. Phys. 56 (1984) 2664.
[5] H.D. Yao, P.G. Snyder, J.A. Woollam, J. Appl. Phys. 70 (1991) 3261.
[6] A.R. Forouhi, I. Bloomer, Phys. Rev. B 38 (1988) 1865.

[7] W.A. McGahan, T. Makovicka, J. Hale, J.A. Woollam, Thin Solid Films 253 (1994) 57.
[8] G.E. Jellison, Jr., F.A. Modine, Appl. Phys. Lett. 69 (1996) 371.
[9] C.C. Kim, J.W. Garland, H. Abad, P.M. Raccah, Phys Rev. B 45 (1992) 11749.
[10] C.C. Kim, J.W. Garland, P.M. Raccah, Phys. Rev. B 47 (1993) 1876.
[11] H. Arwin, D.E. Aspnes, J. Vac. Sci. Technol. A 2 (1984) 1316.